ARTICLE

OPEN

Check for updates

Uncertainty in land-use adaptation persists despite crop model projections showing lower impacts under high warming

Edna J. Molina Bacca [1,2✉], Miodrag Stevanović [1], Benjamin Leon Bodirsky [1,3], Kristine Karstens [1,2], David Meng-Chuen Chen [1,2,4], Debbora Leip [1,2], Christoph Müller [1], Sara Minoli[1], Jens Heinke[1], Jonas Jägermeyr [1,5,6], Christian Folberth [7], Toshichika Iizumi [8], Atul K. Jain [9], Wenfeng Liu [10,11,12], Masashi Okada [13], Andrew Smerald [14], Florian Zabel [15], Hermann Lotze-Campen [1,2,4] & Alexander Popp [1,16]

Climate change is expected to impact crop yields and alter resource availability. However, the understanding of the potential of agricultural land-use adaptation and its costs under climate warming is limited. Here, we use a global land system model to assess land-use-based adaptation and its cost under a set of crop model projections, including CO_2 fertilization, based on climate model outputs. In our simulations of a low-emissions scenario, the land system responds through slight changes in cropland area in 2100, with costs close to zero. For a high emissions scenario and impacts uncertainty, the response tends toward cropland area changes and investments in technology, with average adaptation costs between −1.5 and +19 US$05 per ton of dry matter per year. Land-use adaptation can reduce adverse climate effects and use favorable changes, like local gains in crop yields. However, variance among high-emissions impact projections creates challenges for effective adaptation planning.

[1] Potsdam Institute for Climate Impact Research, Member of the Leibniz Association, Potsdam, Germany. [2] Department of Agricultural Economics, Humboldt-Universität zu Berlin, Berlin, Germany. [3] World Vegetable Center, Tainan, Taiwan. [4] IRI THESys, Humboldt-Universität zu Berlin, Berlin, Germany. [5] NASA Goddard Institute for Space Studies, New York, NY, USA. [6] Columbia University, Center for Climate Systems Research, New York, NY, USA. [7] Biodiversity and Natural Resources Program, International Institute for Applied Systems Analysis, Laxenburg, Austria. [8] Institute for Agro-Environmental Sciences, National Agriculture and Food Research Organization, Tsukuba, Japan. [9] Department of Atmospheric Science, University of Illinois, Urbana-Champaign, Urbana 61801 IL, USA. [10] Center for Agricultural Water Research in China, College of Water Resources and Civil Engineering, China Agricultural University, Beijing, China. [11] National Field Scientific Observation and Research Station on Efficient Water Use of Oasis Agriculture in Wuwei of Gansu Province, Wuwei, China. [12] State Key Laboratory of Efficient Utilization of Agricultural Water Resources, Beijing 100083, China. [13] Center for Climate Change Adaptation, National Institute for Environmental Studies, Tsukuba, Japan. [14] Institute of Meteorology and Climate Research, Atmospheric Environmental Research (IMK-IFU), Karlsruhe Institute of Technology (KIT), Garmisch-Partenkirchen, Germany. [15] Department of Geography, Ludwig-Maximilians-Universität München, Munich, Germany. [16] Faculty of Organic Agricultural Sciences, University of Kassel, Witzenhausen, Germany. ✉email: mbacca@pik-potsdam.de

The land system undergoes continuous adjustments due to the strong dependence of agricultural production on the long and short-term variability of climatic and socio-economic conditions. However, the increasing greenhouse gas (GHG) concentrations are expected to generate unprecedented changes in average local temperatures, precipitation, and recurrence of extreme weather events[1], impacting biophysical factors relevant to crop production[2–4]. Effective adaptation measures, in the form of adjustments to changing ecological and socio-economic conditions, are therefore key to capitalize on possible opportunities effectively and minimize negative impacts[5–10].

Different measures at different system levels can ratchet up agricultural adaptation to climate change. On the farm scale, incremental adjustments in irrigation[11,12], the use of climate-resilient cultivars[13], modifications in planting dates[14], Nitrogen Input[12], and changes in other management practices can improve the resilience of the agroecosystem[15]. To further maximize the benefits of adaptation, a change of production patterns can be introduced at the land-use system scale in the form of transformations between land-use types (e.g., expansion of irrigated and rainfed cropland[16]) or a shift in crop types and cultivation zones within existing crop areas, investments in technological enhancements[10,17], and changes in trade flows[18], among others. Due to the uneven spatial distribution of climate change impacts, a location-specific combination of these measures is required. Additionally, socioeconomic dynamics (e.g., capital allocation) play an essential role in decision-making since they determine relationships between the different levels of adaptation and could slow down the rate at which adjustments are adopted[19].

Most global land system models intrinsically consider various autonomous adaptation measures and their overall effect on food prices, economic welfare, and costs. However, agroeconomic climate change adaptation studies have mainly focused on the analysis of particular adaptation measures (e.g., trade[20–23], cropland expansion[24–26], and investments in research and development (R&D)[27]). Although Iizumi et al.[28] used the CYGMA1p74 crop model and an empirical production function to estimate global adaptation costs at the farm level (maintaining current crop production systems), including CO_2 fertilization, their analysis did not consider transformative changes in land use or regional dynamics. Therefore, there is still a limited understanding of land-use level agricultural adaptation's full potential and associated costs under different scenarios of global change.

Here, we assess the dynamic adaptation of the agricultural production system and its effects under future global change and uncertainty. Our study distinguishes from previous agroeconomic studies on adaptation to climate change in several ways. Firstly, we use the latest multi-model crop yield impact data, including the improvements in crop models since the last Inter-Sectoral Impact Model Intercomparison Project (ISIMIP) round in 2016[29]. Secondly, different from the previous agro-economic literature, we include CO_2 fertilization effects. Prior work only considered limited sources of impact data and simulations that excluded CO_2 fertilization, leading to mostly pessimistic projections of the impacts of the increasing CO_2 concentrations on crop yields and the land-use system. Thirdly, we go beyond existing studies by considering the combined and individual effects of multiple adaptation strategies, such as crop mixes, irrigation investments, and R&D, which go beyond the usual focus on cropland expansion and production relocation. We also account for uncertainty in the response to the impacts and costs of adaptation. Due to its ability to combine spatial biophysical information with the socioeconomic dimension, we use the global land system Model of Agricultural Production and its Impact on the Environment (MAgPIE)[30,31] to evaluate different system-level adaptation measures, their relative importance in the supply-demand balance process, and related costs. The main adaptation measures considered in this study are the relocation of cropping areas (based on socioeconomic and biogeophysical constraints) intra- and internationally (among major world regions), irrigation, cropland expansion, agricultural technological intensification, and shifts in crop mixes grown. We focus on two scenarios. Firstly, a scenario with relatively low emissions and adaptation challenges (SSP1-RCP2.6), and secondly, a high emissions scenario with high challenges (SSP5-RCP8.5). To isolate adaptation effects and measures due to climate change from socioeconomic change, SSP1-RCP2.6 and SSP5-RCP8.5 are compared with SSP1-NoCC and SSP5-NoCC scenarios (baseline scenarios), respectively. In SSPx-NoCC scenarios, MAgPIE calculates land-use adjustments for the specific development (SSPx) trajectories assuming no climate impacts (crop yields and other biogeophysical conditions are kept at 2015 values). Additional details can be found in Table 1 and the Scenarios description subsection of the Methodology. The uncertainty of climate impacts is accounted for by evaluating harmonized and calibrated crop yield data from nine different Global Gridded Crop Models (GGCM) (CYGMA1p74[32], EPIC-IIASA[33], LPJmL[34,35], CROVER[36], ISAM[12], LandscapeDNDC[37], PEPIC[38], pDSSAT[33], and PROMET[39–41]) using five different Climate models (GCM) (GFDL-ESM4, MRI-ESM2-0, UKESM1-0-LL, MPI-ESM1-2-HR, IPSL-CM6A-LR). We use state-of-the-art crop model projections from the phase 3 ensemble of the Agricultural Model

Table 1 Assumptions made in MAgPIE for Shared Socioeconomic Pathways SSP1 (Sustainability) and SSP5 (Fossil-Fueled development).

| Scenario Setting	SSP1 (Sustainability)	SSP5 (Fossil-Fueled development)
Population[71]	Global population grows slowly and peaks in 2050	Global population grows slowly and peaks in 2050
GDP[72]	Rather rapid income growth	Fast income growth and development
Food Scenario[26]	Healthy and low meat diets, reduced food waste	Unhealthy and high meat consumption diets, high shares of food waste
Trade liberalization (% freely located in more competitive regions)	Reaches 20% for livestock and secondary products, and 30% for all other traded commodities in 2050, until 2100	Reaches 20% for livestock and secondary products, and 30% for all other traded commodities in 2050, until 2100
Land protection and afforestation policies	Compatible with the Paris Agreement and the Nationally Determined Contributions (NDCs)	Current National Policies Implemented (NPIs)
Depreciation rate for capital	5%	5%
Bioenergy demand, emissions budget and carbon price[73]	GHG emissions tax emissions and bioenergy demand consistent with an SSP1-RCP2.6 scenario and an emissions budget of 1300 GtCO2 (below 2.0°C) in 2100	Slow incorporation of a uniform carbon price
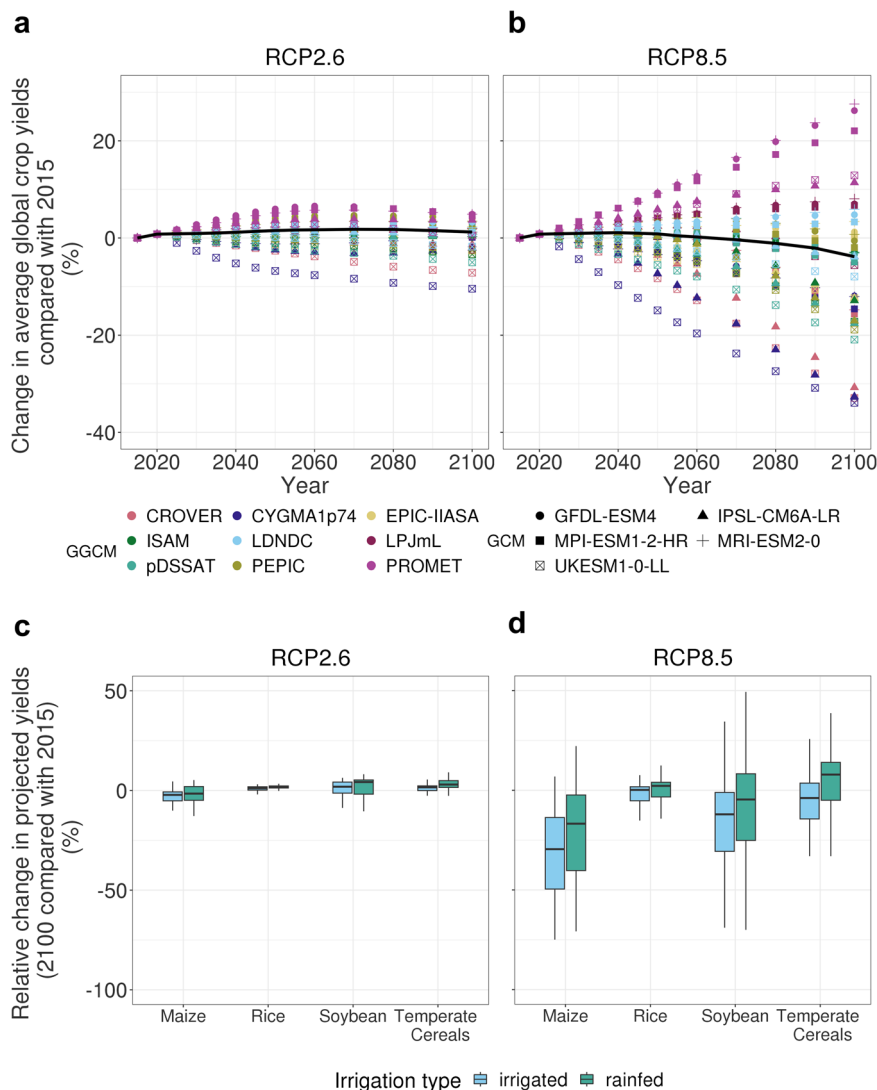
Fig. 1 Global climate change impacts on crop yields under two different emission scenarios. a, **b** Display climate change impacts (relative change of yields compared to 2015 values) on global aggregated crop yields based on harmonized and calibrated crop model projections. Impacts are shown for two different greenhouse gas concentration trajectories, RCP2.6 (low) and RCP8.5 (high-emissions). The yields were aggregated using the cropland patterns and area of 1995. The black line represents the GCM-GGCM ensemble's median value. **c**, **d** Display box plots of the relative change in global average rainfed and irrigated crop yields in 2100 compared to 2015 for the four staple crops (maize, soybean, rice, wheat) and for the GCM-GGCM ensemble of projections. The horizontal solid line represents the median, the box the interquartile range, and the vertical lines extend from the lowest to the largest values of the GGCM-GGCM ensemble.

Intercomparison and Improvement Project (AgMIP)'s Global Gridded Crop Model Intercomparison (GGCMI)[4]. These projections account for CO_2 fertilization effects and the latest climate change data from the Coupled Model Intercomparison Project phase 6 (CMIP6). Detailed information regarding climate change impacts on GCM-GGCM crop yield projections and blue water availability (surface and groundwater reservoirs used for agriculture) can be found in Supplementary Discussion 1 and Supplementary Figs. 1–4.

Results and Discussion
Global land use adaptation and the crop demand-supply balance. For RCP8.5, harmonized and bias-adjusted crop models' projections display large disagreement on the global and regional magnitude and direction of climate change impacts on crop yields (Fig. 1 and Supplementary Figs. 1, 2). This uncertainty increases with GHG concentrations and towards the end of the century. However, in 2100, the median value for the relative change of average

aggregated yields (for maize, soybean, rice, and temperate cereals) for RCP8.5, as compared to 2015, is estimated to be around only −3.8%, being maize and soybean the crop types more sensitive to climate change impacts. Specifically in 2100, taking as reference 2100 SSP5-NoCC's patterns, adaptation for SSP5-RCP8.5 in MAgPIE's GCM-GGCM-based simulations showed (Fig. 2b) a global growth of rainfed cropland area (median = 4.2%, range = [−4.5%,+24%]), a decrease of irrigated area (median = −4.6%, range = [−20%, +33%]), and a slight change of the factor of technological change (TC) (median = +0.23%, range = [−4.2%,+6.6%]). This factor produces a proportional increase in crop yields based on investments in management and R&D[42]. Negative values in adaptation-related changes indicate that projections where yields grow due to CO_2 fertilization (among other phenomena associated with climate change[2]) lead to reduced input requirements compared with SSP5-NoCC. Moreover, our findings display even a lower average cropland expansion required to adjust to climate change in 2100 than previously reported[25] under an SSP5-RCP8.5 emissions and
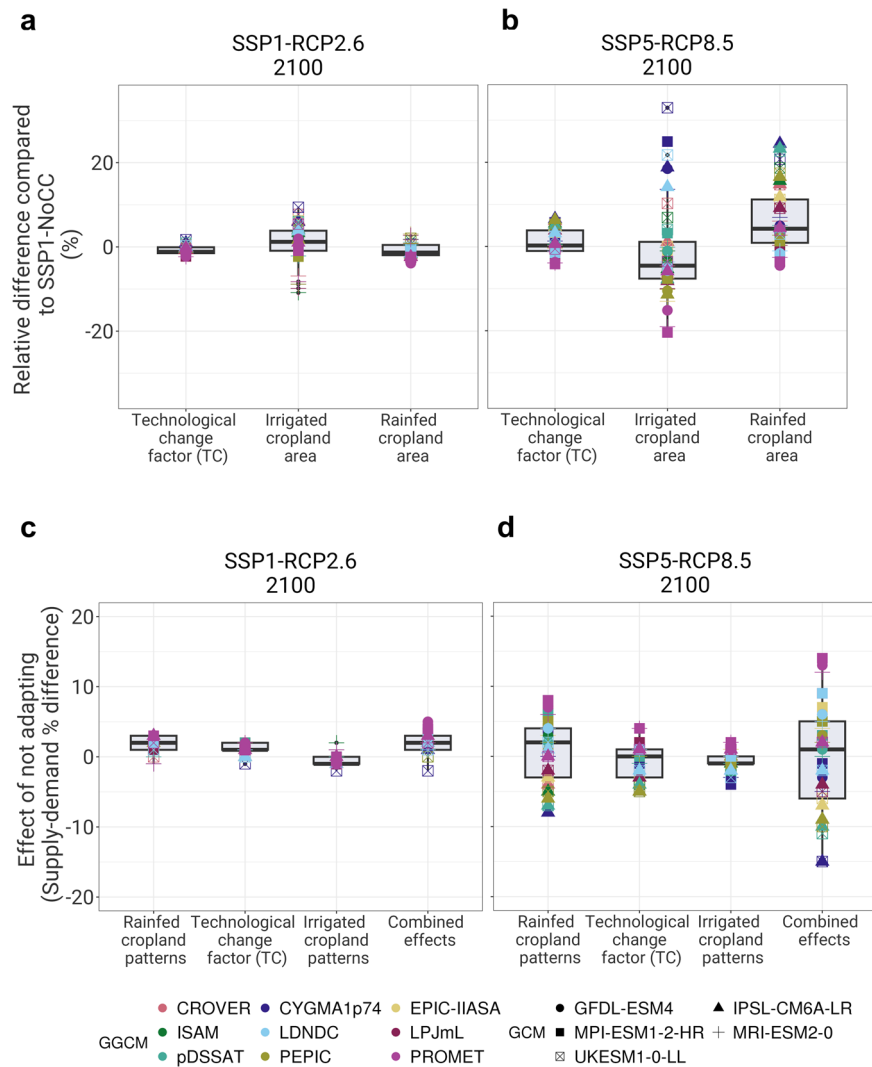
Fig. 2 Global land-use adaptation responses in the MAgPIE model under SSP1-RCP2.6 (low emissions) and SSP5-RCP8.5 (high emissions) scenarios. **a**, **b** Show the relative difference of (TC)* and rainfed and irrigated cropland areas values for SSP1-RCP2.6 and SSP5-RCP8.5 scenarios with respect to the socioeconomic scenarios without climate impacts, i.e., SSP1-NoCC and SSP5-NoCC in the year 2100. **c**, **d** Depict the individual and combined effects of not adapting cropland patterns and TC to climate change. These effects are calculated in a post-processing step as the relative difference between impacted production (calculated using SSPx-NoCC's TC and/or cropland patterns with harmonized and calibrated GCM-GGCM impacted crop yield projections) and SSPx-RCPy demand. *The TC factor produces a proportional increase in crop yields based on investments in management and R&D.

socioeconomic scenario for the year 2050. However, uncertainty remains high. Regarding climate change adaptation for the ensemble of GCM-GGCM-based MAgPIE simulations in 2050, differences between SSP5-RCP8.5 and SSP5-NoCC outputs (TC and cropland patterns) are almost negligible and have a low uncertainty (Supplementary Fig. 5b), compared to 2100.

In a post-processing step, we estimated the impacts of not adapting the land use system to climate change by calculating production using SSP5-NoCC outputs (cropland patterns and TC) and RCP8.5 GCM-GGCM crop yield impact projections for the same year (see the Post-processing calculation of climate impacts on crop production subsection in Methods). This information was then used to estimate the relative difference between the impacted production and the demand. In 2100, not adapting would generate a modest positive overproduction (median = +1%, range = [−15%,+14%]) compared with demand (Fig. 2d). Although overproduction, seen for some GCM-GGCMs simulations, would likely help reduce the risk of food insecurity, it could also impose unnecessary pressure on soils and ecosystems and decrease commodity prices. On the contrary,

in 2050, not adapting displays a slight underproduction (median = −1%, range = [−11%,4%]) (Supplementary Fig. 5d). To better understand the effects of adjusting cropland patterns and TC on balancing supply and demand on the global scale, we calculated, also in a post-processing step, the impact of not adapting these variables (i.e., we used the variables' SSP5-NoCC values) individually while keeping the others at SSP5-RCP8.5 values. Our results display that rainfed cropland patterns exhibit the widest range of effects ([−8%,+8%]) when compared to TC (which ranges from −5% to +4%) and irrigated cropland (which ranges from −4% to +2%) (as shown in Fig. 2d). These results indicate that the climate change impacts on crop yield projections are primarily buffered through adjustments in cropland area and crop mix patterns. However, cropland expansion would induce a self-reinforcing dynamic due to the additional emissions generated by deforestation[43].

Under SSP1-RCP2.6, impacts suggest smaller adaptation challenges than in SSP5-RCP8.5. In 2100, global adaptation would entail a slight increase in irrigated cropland and a slight decrease in rainfed cropland compared with SSP1-NoCC values.

Changes for TC are also lower than for the SSP1-NoCC scenario. Not adapting cropland patterns and TC would result in a slightly higher over-production globally (median = +2%, range = [−2%,+5%]) than SSP5-RCP8.5, which implies that adaptation can also take advantage of positive gains in yields for a more cost-efficient and less intensified production system. 2050's relative change of adaptation strategies, compared with SSP1-NoCC in the same year, is similar to 2100 values but with lower uncertainty.

In general, the positive effects of climate change on yields displayed in some of the simulations of the ensemble of GCM-GGCMs impact data, primarily due to CO_2 fertilization and improved blue water availability, drive reductions in cropland and intensification. This trend aligns with studies considering CO_2 fertilization[20], and differs from studies that ignore it[24]. Under high emissions, if CO_2 fertilization is overlooked, the impacts on yields are primarily negative due to only considering higher temperatures and changes in precipitation during the growing season, which could lead to overestimating the negative average impacts of climate change for certain crops and regions. However, the uncertainty of the impacts of high CO_2 concentrations on crop yields remains high and, consequently, that of adaptation measures. This uncertainty can increase the risk of faulty adaptation planning, also known as maladaptation, which could ultimately exacerbate the situation and leave people and ecosystems more vulnerable to the effects of climate change[44]. Our findings also suggest that the land-use and food systems will need to evolve and increase their flexibility if CO_2 emissions are not reduced.

Regional adaptation to climate change impacts of a high-emission scenario. The global and regional model uncertainty of climate change impacts among the GCM-GGCM ensemble of crop yield projections for the RCP 8.5 scenario increases towards the end of the century. The impacts' range leads to very different intra- and inter-regional adaptation dynamics within the GCM-GGCM-based MAgPIE simulations. To exemplify the disparity of land-use adaptation that could take place for an SSP5-RCP8.5 future, we evaluate the relative difference between three MAgPIE GGCM-GCM-based simulations and SSP5-NoCC in the year 2100 for TC, rainfed and irrigated cropland, crop mixes and production allocation (absolute global and regional time series can be found in Supplementary Figs. 6–9). Specifically, we describe the regional adaptation strategies for the LPJmL-MRI-ESM2-0 combination, given that this GCM-GGCM contains all the crop types used in MAgPIE. Additionally, regional adaptation strategies simulated by MAgPIE are also described for the GCM-GGCM combinations located at the extremes of the range of the global average crop yield projections in 2100 (Fig. 1b) (CYGMA1p74-UKESM1-0-LL as the most pessimistic, and PROMET-MRI-ESM2-0 the most positive).

The global adaptation response under the LPJmL-MRI-ESM2-0 projection includes smaller irrigated (−10%) and slightly larger rainfed (+0.3%) cropland areas in 2100 compared to SSP5-NoCC. In this case, moderately lower TC (−1.1%) is also seen (Fig. 3). A likely cause is the water-saving effect of CO_2 fertilization leading to higher rainfed yields, reducing the relative benefits of irrigation compared to rainfed production.

Regionally, under this GCM-GGCM simulation, the reforming economies (REF) experience the highest relative change in domestic livestock (+26%) and crop (+12%) production compared with SSP5-NoCC, which in consequence, increases its self-sufficiency ratio (SSR) (from 0.98 to 1.06) under climate change (Fig. 4). The SSR represents, in value terms, the fraction of demand for traded agricultural commodities that are produced

domestically (see the Self-sufficiency ratio (SSR) subsection in Methods). Increased livestock exports explain this growth which is backed by an increase in crop yields (yields including adaptation) (rainfed +11%, irrigated +3.3%) and water availability for agriculture (Supplementary Fig. 4). Associated with the comparative advantages of producing livestock products in REF, we see a lower livestock production in large producing regions such as the countries of the European Union (EUR) (−3.2%) and the United States of America (USA) (−5.6%). Compared with SSP5-NoCC, EUR experiences a decrease in irrigated yields (yields including adaptation as TC and crop mixes changes) (−17%), which increases the need for cropland (rainfed = +3.4%, irrigated = +4.5%), reducing the area available for pastures. Regarding the largest producers, Latin America (LAM) and Other Asia (OAS) experience a slightly lower overall crop production (LAM = −3.2%, OAS = −1.3%) due to gains in competitiveness in other regions in 2100 (Supplementary Fig. 10). This causes slight negative relative differences in irrigated (LAM = −14%, OAS = −1%) and rainfed cropland (LAM = −5%, OAS = −3%) and in the self-sufficiency ratio (LAM = −2, OAS = −1 percentage points) compared with SSP5-NoCC. As for the differences in cropping patterns, the largest shifts in the relative crop mixes grown (Fig. 5b) are seen in the Sahel region (85%) and Equatorial Africa (64%), changes occur due to a reduction of maize production (relocation to more competitive regions) that turns in higher shares of other crops; in parts of Afghanistan and Pakistan (70%) also due to the relocation of production of maize and a subsequent higher share of temperate cereals; and in the Mediterranean Region (65% of the mix is different from SSP5-NoCC), mostly due to the relocation of temperate cereals to higher latitudes and a higher share of maize. Although LPJmL-MRI-ESM2-0 does not show large global average impacts on yields, these changes in crop mixes highlight how climate impacts on agriculture are predominantly experienced at the local level and indicate that the affected communities would need to undergo considerable adjustments to stay competitive. More details about how the shift in crop mixes was calculated can be found in the Methods' subsection Shifts in crop mixes grown.

On the negative end of average climate change impacts, MAgPIE's simulation based on CYGMA1p74-UKESM1-0-LL crop yield projections, contrarily to LPJmL-MRI-ESM2-0, displays a positive relative difference in the factor of technological change (TC = +6%) and cropland (irrigated = +32%, rainfed = +21%) to meet future crop demand compared to SSP5-NoCC in 2100.

Regionally, the USA, despite adaptation responses (TC = +4%, rainfed cropland = +15%, and irrigated cropland = +103%), experiences the largest drop in crop production (−34%) (Supplementary Fig. 10a) of all regions compared with SSP5-NoCC in 2100. Consequently, its self-sufficiency ratio gets reduced due to fewer crop and livestock exports. Similarly, negative relative differences in crop production occur in India (IND) (−17%), Canada (CAN) (−12%), and China (CHA) (−5%) despite higher investments in technology (CAN's TC = +24%, IND's TC = +7.6% and CHA = +6.9%), and higher rainfed (CAN = +14%, IND = +17%, CHA = 21%) and irrigated (CAN = +357%, IND = +1.7%, and CHA = +132%) cropland area. Some regions with a resulting large decrease in estimated yields, such as Latin America (LAM) (irrigated = −48%, rainfed = −23%) and Sub-Saharan Africa (SSA) (irrigated = −65%, rainfed = −10%), increase their domestic crop production (LAM = +6.3%, SSA = +5.6%) through larger cropland area in contrast to SSP5-NoCC. The extended crop yields decline in all regions and LAM's and SSA's low land conversion and production costs (compared with other regions) could explain this counter-intuitive behavior. Regarding crop mixes (Fig. 5a),
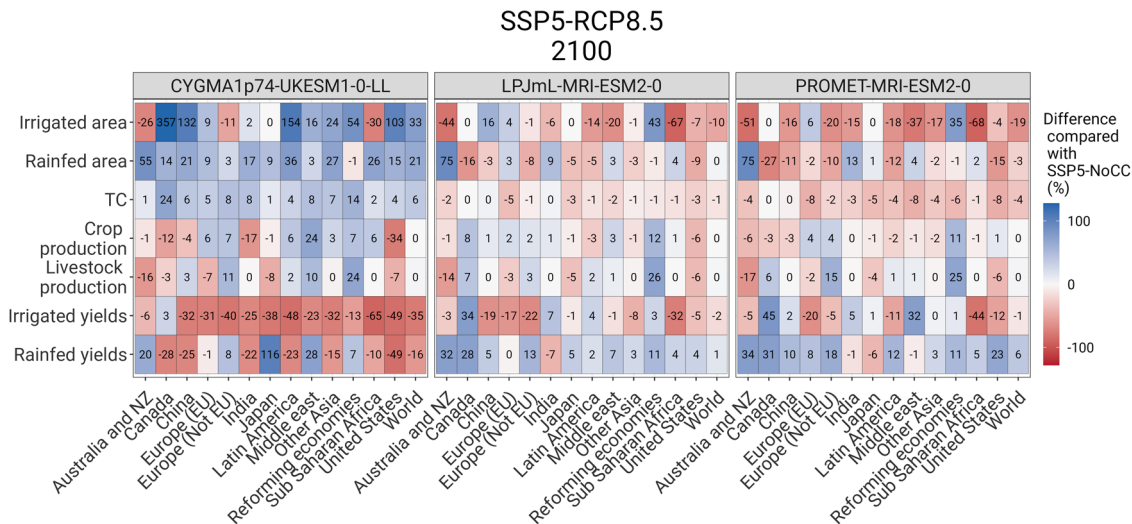
SSP5-RCP8.5
2100

Fig. 3 Regional relative difference of adaptation-related variables estimated by MAgPIE in the year 2100 for three different GCM-GGCM combinations, compared to the SSP5-NoCC scenario (without climate impacts). The color of the tiles represents the relative difference between the SSP5-RCP8.5 simulations and the SSP5-NoCC scenario (red for lower than zero and blue for larger than zero values) for the year 2100. The numbers represent the exact values. Production, (crop) areas (irrigated and rainfed), and (crop) yields refer not only to the four staple crops (maize, soybean, rice, and temperate cereals) but to the 19 types considered in MAgPIE. TC corresponds to the technological change factor that produces a proportional increase in crop yields based on investments in management and R&D. Yields reported here include the effects of adaptation. Specifically, three GCM-GGCM combinations are presented, CYGMA1p74-UKESM1-0-LL (most negative average global impacts), LPJmL-MRI-ESM2-0 (MAgPIE's default GCM-GGCM combination), and PROMET-MRI-ESM2-0 (most positive average global impacts).
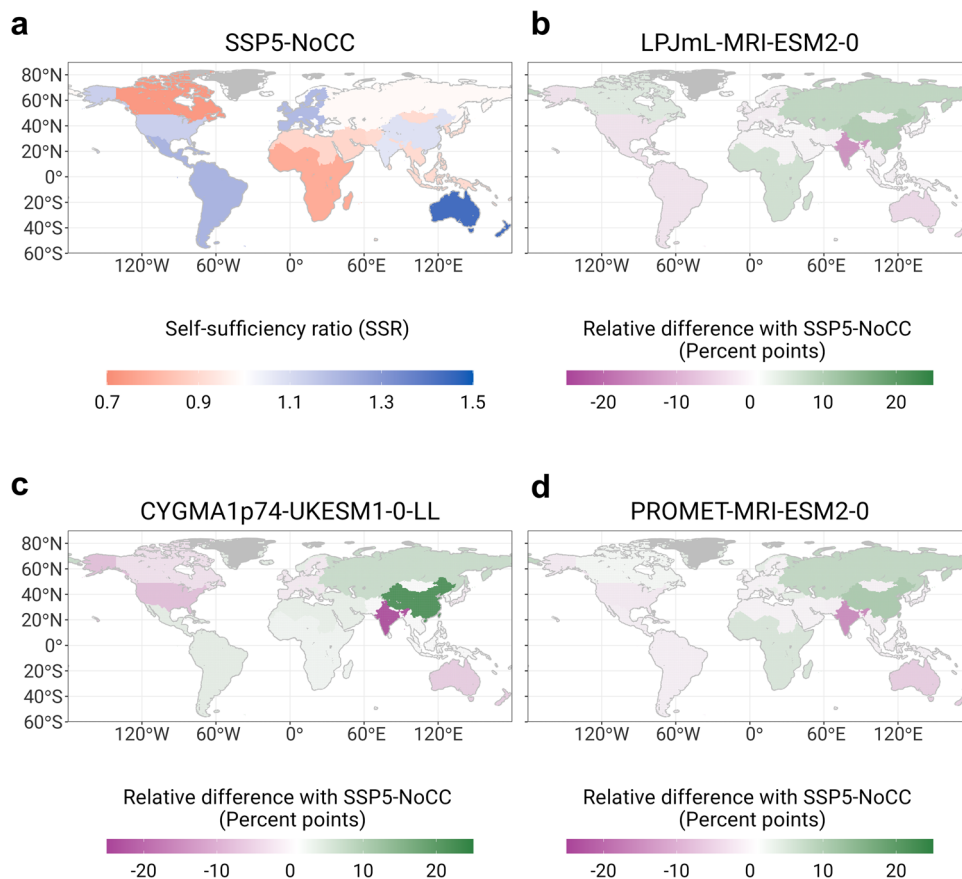
Fig. 4 Aggregated self-sufficiency ratio of traded agricultural products and their relative percentual change compared with the SSP5-NoCC scenario. Values are plotted by world region for the year 2100 under the most divergent scenarios in SSP5-RCP8.5, and LPJmL-MRI-ESM2-0. **a** SSP5-NoCC self-sufficiency ratio, **b** LPJmL-MRI-ESM2-0, **c** CYGMA1p74-UKESM1-0-LL, **d** PROMET-MRI-ESM2-0 represent the difference in percentage points of the self-sufficiency ratio between the SSP5-RCP8.5 simulations and SSP5-NoCC.

a

CYGMA1p74-UKESM1-0-LL

b

LPJmL-MRI-ESM2-0

c

PROMET-MRI-ESM2-0

Shift of cropland allocation among crop types
(percentage points)

0   25   50   75   100

Fig. 5 Shift (in percentage points) of allocation of cropland among different crop types for the SSP5-RCP8.5 scenario, three different GCM-GGCM combinations and compared to the baseline sceneario SSP5-NoCC (no climate impacts) in 2100. Specifically, for (**a**) CYGMA1p74-UKESM1-0-LL (most negative average global impacts), (**b**) LPJmL-MRI-ESM2-0 (MAgPIE's default GCM-GGCM), and (**c**) PROMET-MRI-ESM2-0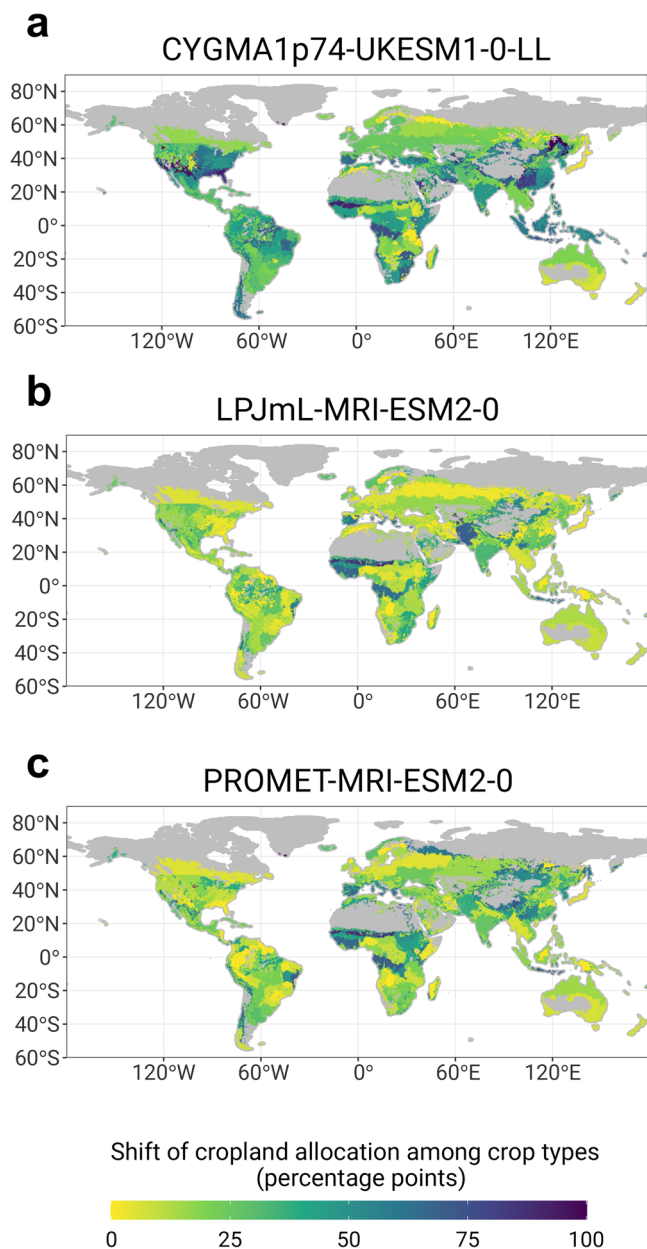 (most positive average global impacts). Yellow areas (0 percentage points) show that the distribution (in %) of cropland among crop types is the same between the GCM-GGCM MAgPIE simulation and SSP5-NoCC. Dark blue (100 percentage points) indicates that cropland was distributed among a completely different crop mix compared to SSP5-NoCC.

shifts are driven primarily by losses in maize yields in the USA and CHA, resulting in up to 90% changes in crop shares in these regions compared to SSP5-NoCC in 2100. LAM, particularly in Brazil and Chile, displays higher shares of maize and soybean at the expense of temperate cereals and rice. In SSA, the Sahel region displays a larger share of maize production, while Equatorial Africa experiences a decrease, indicating internal regional relocation of production. OAS (specifically, insular South East

Asia) and EUR (Mediterranean Region) also shift towards higher shares of maize by relocating other crops like temperate cereals.

Finally, on the positive end of impacts, the PROMET-MRI-ESM2-0 simulation is characterized by large increases or slight decreases in crop yields in most regions. Accordingly, this simulation exhibits a lower global need for cropland (irrigated = −19%, rainfed = −2.6%) and investments in R&D (TC = −4%) in 2100. Smaller TC and cropland are also seen in almost all regions compared with SSP5-NoCC. Regarding domestic production of crops and livestock, most of the regions only experience minor differences. Australia and New Zealand (ANZ), REF, and European countries not in the EU (NEU) are the only ones that stand out due to their relative crop (ANZ = −6%, REF = +11%, NEU = +4%) and livestock (ANZ = −17%, REF = +25%, NEU = +14%) production changes. Regarding crop mixes, the gains in crop yields, particularly in soybean, temperate cereals, and maize, result in changes in the proportion of crops grown in different regions, once again, most notably in the Sahel (85% shifted) Region and Equatorial Africa (76%), the Mediterranean region (70%), as well as specific areas in Brazil (up to 70%) and Chile (up to 70%).

Although there is a large disparity in the projected distribution of impacts on the regional scale among the ensemble, our results indicate that while high-latitude regions like NEU and REF may experience an increase in crop production in a high-emissions scenario, they would remain small producers compared to LAM, OAS, or EUR (as illustrated in Supplementary Fig. 10). Even in scenarios where most regions face a decline in crop yields, LAM, SSA, or OAS still increase their production by expanding cropland. These regions contain biodiversity hotspots, so cropland expansion driven by climate change could threaten these already fragile ecosystems[39]. Our findings also show the critical role that local and regional adaptation plays in facing (or taking advantage of) climate change impacts. Particularly, the cropland allocation among crop types in the Sahel, Equatorial Africa, and the Mediterranean regions is notably sensitive to variations in crop yields due to climate change.

Costs of adaptation to climate change. Global average adaptation costs (see Costs related with adaptation in Methods) for crop production and their uncertainty concerning crop model projections differ greatly between the SSP1-RCP2.6 and SSP5-RCP8.5 scenarios (Fig. 6) in 2100 for the GCM-GGCM ensemble. SSP5-RCP8.5 displays yearly positive average global adaptation costs (average = +4.8 US$05 per ton of dry matter, range = [+19, −1.5] US$05 per ton of dry matter). Positive (negative) adaptation costs indicate increased (decreased) production costs under SSP1-RCP2.6 and SSP5-RCP8.5 relative to the non-climate change scenarios, SSP1-NoCC and SSP5-NoCC in each year, respectively. For the estimated global crop production in 2100 under an SSP5-RCP8.5 developing trajectory, this uncertainty translates into absolute production adaptation costs ranging between −17 and 209 billion US$05 per year. Although the values cannot be directly compared due to methodological differences, previous farm-level studies such as that of Iizumi et al.[28] projected only positive adaptation costs between 91 and 94 billion US$05 per year for the 2091–2100 decade under high emissions and impacts on four staple crops (maize, soybean, rice, and wheat).

In an SSP1-RCP2.6 world, global average climate change adaptation costs are almost zero (average = +0.31 US$05 per ton of dry matter, range = [−0.62, +1.4] US$05 per ton of dry matter]) in 2100. However, uncertainty in yearly adaptation costs for SSP1-RCP2.6 is highest in the year 2050 (average = −4 US$05 per ton of dry matter, range = [−10,2.5] US$05 per ton of dry
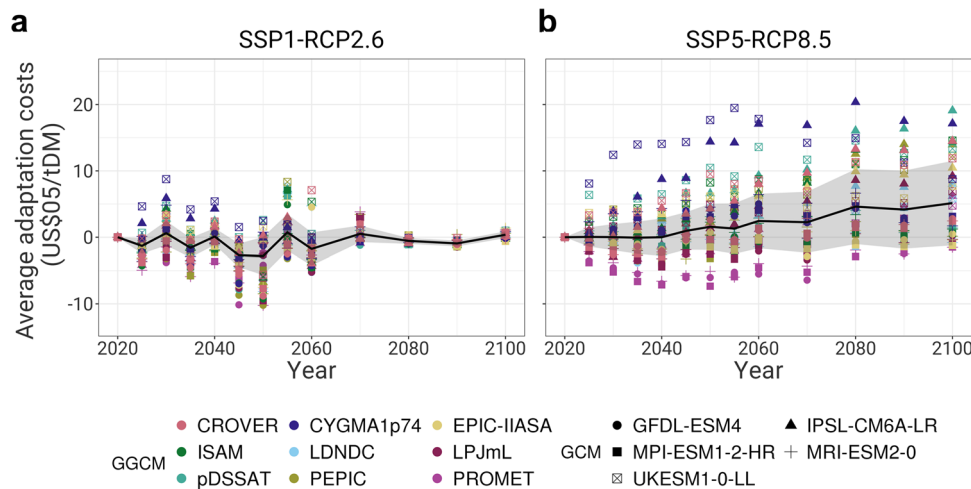
Fig. 6 Global climate change-driven adaptation costs for crop production for SSP1-RCP2.6 and SSP5-RCP8.5 and for the ensemble of GCM-GGCM. **a**, **b** Show climate change-driven adaptation costs for the multi-model ensemble of runs for SSP1-RCP2.6 (low emissions) and SSP5-RCP8.5 (high emissions) scenarios, respectively. The black line represents average values, while the shaded area is the standard deviation).

matter). The higher uncertainty projected in 2050 can be attributed to the adaptation driven by a peak in population in 2050. This results in a higher demand for agricultural commodities in 2050 compared to the second half of the century. For the socioeconomic scenarios SSP1 and SSP5, a decrease in population in the second half of the century also suggests that after 2050 the food system will primarily need to address the impacts of climate change and dietary choices rather than an increase in demand, implying that after 2050 the food system will rather have already established infrastructure to produce more than what will be demanded in the second half of the century, mitigating part of the uncertainty in costs associated with crop yield projections.

The results for SSP5-RCP8.5 suggest no large reductions in production costs for those GCM-GGCM with gains in crop yields in 2100. They also suggest that the growth in costs and their uncertainty are associated with differences in investments in intensification (average = +1.3 US$05 per ton of dry matter, range = [0,+5.5 US$05 per ton of dry matter]) and land conversion to cropland (average = +2.4 US$05 per ton of dry matter, range = [−1 US$05, +13 US$05 per ton of dry matter]). Although the changes and uncertainty in land conversion costs were expected, the behavior of investments in intensification implies high marginal costs for this adaptation mechanism compared with the others.

For the SSP5-RCP8.5's GCM-GGCM combinations at the extremes of the range of average projected climate impacts on yields, a reduction in production costs (−1.3 US$05 per ton of dry matter) was calculated for PROMET-MRI-ESM2-0 (largest gains in projected yields) due to lower conversion, trade & transport, and intensification costs compared to SSP5-NoCC. In contrast, an increase of +9.8 US$05 per ton of dry matter in cost is seen for CYGMA-UKESM1-0-LL (Figs. 6, 7). Although CYGMA-UKESM1-0-LL displays the largest losses in global average yields projections of the GCM-GGCM ensemble in 2100, pDSSAT-IPSL-CM6A-LR shows the highest average costs of adaptation (+19 US$05 per ton of dry matter), specifically due to larger land conversion in the USA compared to SSP5-NoCC. Our findings indicate that regional climate change impacts dynamics, the rate of change, and previous land-use adjustments have a larger effect on costs than the global averaged impacts in one specific year. More information about regional adaptation costs can be found in Supplementary Fig. 11.

Limitations. Our study explores how the land-use system might adapt to climate change's impacts without radical transformations to the economic and food production systems (e.g., degrowth, and cultivated meat, among other exciting developments still not introduced at large scale or not yet conceived). Given that there is still much uncertainty around the impacts of climate change on crop yields (additional information about the sources of variance, including a sensitivity analysis for MAgPIE's assumptions, can be found in Supplementary Discussions 2 and 3) and the increase in atmospheric CO_2 concentrations, our goal is to analyze the range of potential futures that the land-use system could face under different emissions scenarios, using the most up-to-date impact data available. However, it is important to note that the average values presented in our study should not be misinterpreted as the most probable future. Consequently, our work is not intended to provide fixed adaptation mechanisms or advise policymakers. We aim to contribute to a better understanding of the system's boundaries regarding adaptation mechanisms and capacities considering the interaction between global and regional scales.

Regarding additional limitations, the impact data generated by the GCM-GGCM model only considers four staple crops, which account for two-thirds of human caloric intake[45].

Although LPJmL impact data was used for the remaining crop types and no inconsistencies are expected (the four modeled crops are independently modeled from other crops and were not grouped with other crop categories in MAgPIE), this impact data only shows variance across GCMs. Given the high variance of impacts from crop models, our output parameters, which depend on the aggregate impacts of all crops (such as land expansion), only capture some of the cross-model differences. Moreover, LPJmL is one of the GGCMs with a relatively optimistic outlook regarding crop yield projections. This suggests that, for additional crops, projections may be less pessimistic than those produced by other GGCMs. Previous impact studies have mainly focused on the impacts of climate change on wheat, maize, soybean, and rice, which means that there may be even greater uncertainty around the impacts of climate change on other crop types. More information about this and possible future actions to address the issue can be found in Müller et al.[46].

In the specific GCM-GGCM impacts data set here, farm-level management decisions (e.g., changes in growing dates, and nitrogen input, among others) are underrepresented, which could lead to underestimating adaptation potentials for the overall
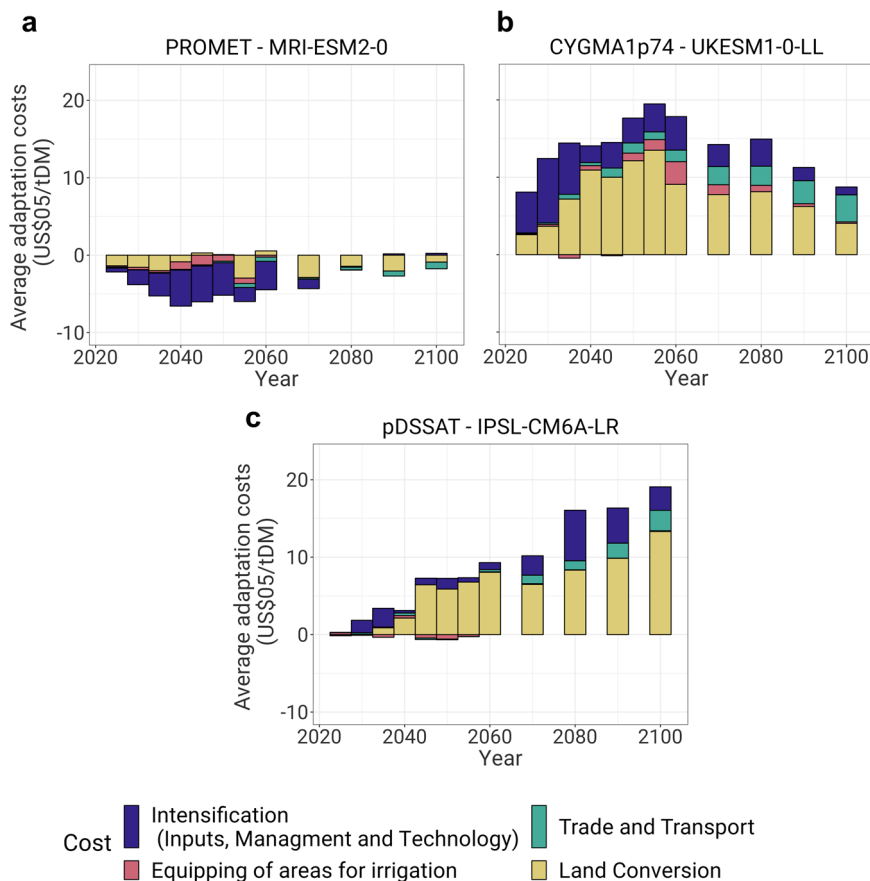
Fig. 7 Details of Climate change-driven adaptation costs for crop production. The figure displays, compared to SSP5-NoCC the details of the changes in specific adaptation-related costs in dollars per tonne of dry matter (tDM), for crop production and for the most expensive and the most divergent, in terms of biophysical impacts, GCM-GGCMs. Specifically, (**a**, **b**) show costs for the SSP5-RCP8.5 (high emissions) scenario for PROMET-MRI-ESM2-0 and CYGMA1p74-UKESM1-0-LL, respectively, and (**c**) shows details for the GCM-GGCM with higher adaptation costs in 2100 (pDSSAT-IPSL-CM6A-LR).

agricultural system. For this reason, future analyses could include parallel farm- and land-use level adaptation to estimate the full potential of the agricultural sector. Another limitation is that we focus on autonomous land system-level adaptation, i.e., on those system measures at local and global scales that emerge as market responses to climate change-driven disturbances in crop yields and resource availability. Although we include bioenergy, afforestation, and protection policies associated with the socio-economic trajectories of the scenarios SSP1 and SSP5 (see Table 1), future work should also consider strategies under planned adaptation. For example, more stringent policies could be included to evaluate additional pressures to the system like preservation and expansion of protected areas, ensuring calorie availability for consumers (via subsidies)[21], or stimulating rural development[47]. Considering more drastic policies such as land protection schemes could constrain adaptation potentials and favor environmental benefits at the expense of, most likely, higher costs due to the need for higher investments in capital and technology, irrigation, or relocation to expensive production areas. Since we focus on global and long-term impacts, other dynamics missing in our analysis include extreme weather effects, the uncertainty of the impacts that geopolitical instabilities[48] or other socioeconomic scenarios could have on commodity prices and trade flows. Finally, we did not consider other scarcely reported effects on crop production, such as the impact of heat stress on labor and animal productivity.

To conclude, our main findings indicate that considering the effects of CO_2 on crop yields could result in a lower required global expansion of cropland (based on median values) and cropland intensification and, consequently, lower adaptation costs than previously reported to adjust to climate change. However, there remains a high level of uncertainty regarding land-use adaptation measures at the global and regional scales. We also found that adaptation costs, towards the end of the century, would not depend on the average global impacts but rather on the regional distribution of effects, the rate of change, and previous adjustments made to the system based on socioeconomic drivers of change. That is to say that the large range of possible impacts and, in consequence, adaptation mechanisms as GHG emissions increase highlight the need for a more flexible food system on both the supply and demand sides. This could involve introducing new technologies, creating more liberalized markets[20], and implementing more profound transformations to the economic system[49], among other measures.

Methods

MAgPIE model. The MAgPIE land system modeling framework (Version 4.4.0) is an open-source, recursive dynamic global partial equilibrium model[30,31] for the agricultural, forestry, and other landuse (AFOLU) sectors. The model minimizes the overall AFOLU costs based on spatially-explicit agricultural productivity values, the demand for agriculturally-based food, feed and material demand, and international trade[30,50]. The projections of socioeconomic drivers such as population, development state, and demography are carried out in this study on the level of 13 socioeconomic regions (Supplementary Fig. 12). The scenario parametrization is based on the Shared Socioeconomic Pathways database (SSPs)[51]. The demand for food and its various components is projected by considering population growth, demographic structure, and per-capita income. Factors such as household food waste, body height, body weight, and physical activity levels are also considered

(more information can be found in Bodirsky et al.[52]). In this study, food demand is assumed to be price inelastic. Bioenergy demand is estimated as the combination of 1st generation biofuel demand in the shorter term and a longer-term demand for 2nd generation biofuels (derived from previous studies through coupling with the REMIND model)[53]. Livestock demand is estimated using exogenous region-specific feed baskets and productivity, influencing crop demand for feed use. Then, the distribution of livestock production is linked to subregional fodder, pasture, and urban areas. Trade is calculated based on historical region-specific patterns and comparative advantages in production costs among regions. Specifically, the model allows for assessing climate effects on the AFOLU sector through simulated changes in yields, water availability and crop irrigation requirements, and soil carbon. The biophysical constraints used in MAgPIE for the evaluation of different climate futures are usually derived from the Lund-Potsdam-Jena managed Land (LPJmL) dynamic global vegetation model[34,35,54] which simulates crop yields, and other biophysical and biogeochemical processes for different major crops, pastures, and rangelands under different climate scenarios at gridded resolution (0.5° × 0.5). In this study, high-resolution crop yields are used from an ensemble of different crop models (pDSSAT, EPIC-IIASA, CYGMA1p74, CROVER, PROMET, Land-scapeDNDC, PEPIC, ISAM, and LPJmL) (see below for more information about sources, harmonization, and calibration of MAgPIE's biophysical inputs from the crop models). Additional carbon stocks, water availability, irrigation water demand for crops, and pasture climate impact data come from LPJmL simulations. The gridded inputs regarding potential yields, water availability and requirements, and terrestrial carbon content are then aggregated to 200 (default setting) clusters based on the k-means clustering method and on yields, irrigation, and transport distance similarity criteria[30]. Each cluster is assigned to one of MAgPIE's socioeconomic regions.

Regarding the optimization process, the minimization of production costs is carried out for each time step under consideration. The current analysis was carried out between 1995 and 2100 in time steps of 5 years until the first half of the 21st century and ten years in the second. More details about MAgPIE's parametrization of processes related to adaptation, and a sensitivity analysis in which the impacts of related assumptions are assessed, can be found in Supplementary Methods 1 and Supplementary Discussion 3.

Costs related with adaptation. Concerning costs related to adaptation, we focus on four cost categories in MAgPIE. Firstly, land conversion costs estimate the costs of converting between different land cover types, specifically for expanding cropland, pasture, and forests. For cropland, a reward for reduction is also considered. Given the lack of information regarding cropland reduction costs, MAgPIE counts with a calibration routine to find the regional costs that best match historical land cover trends. Secondly, we evaluate intensification costs, including input factors (labor and capital requirements) and investments in management and technology. The investments destined to improve technology and management practices are translated into a landuse intensity factor (TC), which proportionally increases MAgPIE's calibrated yields[42]. Input factor costs in MAgPIE depict the requirements for capital and labor per crop and region. We assume that costs associated with labor are fixed per tonne of crop type produced. For capital, we consider investments to be dependent on previous capital stocks and their depreciation and specific for each crop type produced. In consequence, input factor costs represent shifts in the crop types produced within a cluster cell as an adaptation measure. Fertilizer and chemicals costs are considered in other modules in MAgPIE. Thirdly, the costs of equipping areas for irrigation account for the required investments needed to expand and equip irrigated cropland. Finally, trade and transportation costs are accounted for in our results. Transportation costs are based on the costs of moving agricultural commodities intra-regionally between production sites and the closest market center. Trade costs are based on the regional net exports (and their specific trade margins and tariffs per region and commodity) for traded products (crops, distilled products, fibers, livestock products, oil cakes, and molasses).

Adaptation costs are then calculated as the absolute differences of these costs (aggregated) between the scenarios with climate impacts (SSP1-RCP2.6 and SSP5-RCP8.5) and the corresponding costs for the scenarios without climate effects (SSP1-NoCC and SSP5-NoCC). This ensures the isolation of the costs related to climate change adaptation without the adjustments made due to socioeconomic development pressures. Finally, we divide the adaptation costs by the aggregated crop production (tDM) to determine the average adaptation costs per unit of crop produced.

Scenarios description. To comprehensively analyze climate change impacts and adaptation strategies in agriculture, we evaluate two different climatic futures with their corresponding socioeconomic trajectory and uncertainties. From the climate perspective, RCP scenarios were constructed to evaluate possible futures concerning concentrations of GHG (climate forcing agents)[55]. RCPs are named and based on their target level of radiative forcing for the year 2100. They are often paired with consistent socioeconomic trajectories stemming from the SSP scenarios.

The SSP narratives entail a broad selection of baseline assumptions of socioeconomic variables (demographic, economic, technological, social, governance, and environmental) to account for the uncertainty of possible development paths[51,56].

From the modeling-chain perspective[25], general circulation/earth system models (GCM) take the information of the RCP trajectories (GHG concentrations) to estimate their effects on climate variables (such as temperatures and precipitations). The global gridded crop models (GGCMs) then use the data on climate variables to evaluate their impact on biophysical variables (such as crop yields, soil carbon, water demand, and availability). Finally, the outputs from the crop models become inputs, together with the SSPs assumptions on population, GDP, and food demand, among other economic constraints, for the economic models (such as MAgPIE). A detailed flow diagram of the modeling chain can be found in Supplementary Fig. 13.

In our study, we focus on two different climate-socioeconomic scenarios. A sustainable low-emission scenario with low adaptation challenges (SSP1-RCP2.6) and a resource-intensive high-emission (SSP5-RCP8.5) one to cover the overall range of possible impacts.

The SSP1 scenario[51], describes a relatively sustainable development pathway; effective cooperation of organizations (local, national, and international) and sectors (institutions, private, and civil society); lower population growth; modest and greener economic growth with a rapid convergence of lower-income countries; and reduction of resource-intensive lifestyles, and measures to improve the efficiency of production. For land use and the food system[26], SSP1 represents a world where land and deforestation are highly regulated, with healthy and low-meat consumption diets and low food waste rates. SSP1 is matched here to RCP2.6, which represents a forcing level in line with a warming level below 2° Celsius at the end of the century and compared with pre-industrial levels[1]. The SSP5[51] scenario displays rapid growth of emerging and industrialized economies, integration of global markets, innovative and participatory societies that invest in social and human capital, and the removal of institutional barriers. This "highway" road is characterized by exploiting fossil fuels, resource-intensive lifestyles, and local solutions to environmental impacts through technological advancements. It also assumes limited cooperative intention to solve global environmental concerns. Population peaks and then slowly declines in the middle of the 21st century. In this scenario, diets are unhealthy, with high animal consumption and high food waste shares. SSP5 is paired to RCP8.5, which displays high radiative forcings due to a steep growth of GHG emission and concentrations and a warming level of above 4° Celsius at the end of the century, compared with pre-industrial levels[1].

To determine adaptation due to only climate change and not socioeconomic adjustments, SSP1-NoCC and SSP5-NoCC runs were also made. In the SSPx-NoCC runs, socioeconomic assumptions corresponding to the SSP1 and SSP5 trajectories were used, but biophysical data were assumed to stay constant at 2015 values throughout the century. Finally, although the response analysis primarily centers around 2100 values, 2050 values are also considered on the global scale. This is because, based on Müller et al.[46], during the first half of the century, differences in parametrization and modeling assumptions of biophysical processes largely dominate the variance in crop yields among the GGCMs. However, in the second half of the century, the climate signal becomes larger, and its uncertainty plays a more prominent role.

Source of biophysical impacts data. To evaluate the uncertainty of climate change adaptation measures and costs in agriculture, we use a set of GCM-GGCM crop yield projections for the different climate-socioeconomic scenarios (SSPs-RCPs). For this purpose, we use the data reported in phase 3b of the Inter-Sectoral Impact Model Intercomparison Project (ISIMIP)[57]. ISIMIP provides a consistent framework to evaluate possible climate change impacts for diverse sectors and scales under common climate and forcing data, scenarios set-up, terms of data, and format. The results of each evaluation round are made available to be used by the scientific community[58]. Within the ISIMIP3b simulation round, RCP2.6, RCP7.0 and RCP8.5 are assessed by different global gridded crop models for five different GCM climate forcing datasets (GFDL-ESM4, MRI-ESM2-0, UKESM1-0-LL, MPI-ESM1-2-HR and IPSL-CM6A-LR). The climate forcing datasets were bias-adjusted and statistically downscaled based on the CMIP6 framework and methods for the consistent intercomparison of climate models[59–61]. Within our study, we specifically focus on the RCP2.6 and RCP8.5, as they represent the full range of climatic futures available within the available ISIMIP 3b sets.

We used LPJmL, EPIC-IIASA, pDSSAT, CYGMA1p74, PEPIC, PROMET, CROVER, LandscapeDNDC, and ISAM crop yield projections. We selected these models because they reported information for the four crops (maize, soybean, rice, and wheat) and five climate models here considered. These sets are outputs of the AgMIP's Global Gridded Crop Model Intercomparison (GGCMI) framework[4]. ISIMIP3b only provides yield projections for a limited number of staple crops (maize, soybean, winter wheat, spring wheat, and two rice seasons). These crops were mapped to MAgPIE's maize, soybean, rice, and temperate cereals crop types. Winter and spring wheat and the different rice types were merged and mapped to temperate cereals and aggregated rice via a cultivated area mask, available via the ISIMIP3b database. Wheat represents the bulk of temperate cereals, and rice, soybean, and maize are part of MAgPIE's 19 crop types. Given that these four staple crops cover nearly two-thirds of global agricultural consumed calories[62], we assume that they can represent the bulk of climate change impacts on the global food system. The data was also harvest-year corrected to make sure that the harvest year reported by the GGCMs corresponded to calendar years. Specifically, when the maturity day of a crop took place before the planting date, we assumed that the reported crop yield value corresponded to the following year's harvest.

Since MAgPIE evaluates 15 additional crop types beyond the four major staples, it was necessary to use LPJmL yields for the missing crop types. Additional climate impacts data regarding carbon stocks (vegetation, litter, and soil) and water availability were simulated for the different GCMs using LPJmL4[54], and yield and irrigation water demand data for additional crops and pasture were simulated using LPJmL5, which is the same version used for CMIP6.

In total, 45 combinations of GCM-GGCM projections were calibrated and harmonized for each SSPx-RCPy scenario, as explained below. These combinations are the result of using the nine crop models and five different General Circulation Models (GCMs) (GFDL-ESM4, MRI-ESM2-0, UKESM1-0-LL, MPI-ESM1-2-HR, IPSL-CM6A-LR). The analysis of impacts shown in Supplementary Discussion 1 corresponds to the aggregated potential yields of the four staple crops (maize, soybean, temperate cereals, and rice). The global averages were aggregated using constant 1995 cropland patterns as weight.

Climate trends extraction and historical harmonization of biophysical inputs. Spatially explicit biophysical constraints in MAgPIE are usually derived from simulated data by the dynamic global vegetation, crop, and hydrology model LPJmL at a spatial resolution of 0.5 degrees (latitude/longitude) and driven by historical climate data time series[63]. In this study, to assess uncertainty, crop yield patterns from other global gridded crop models are also considered and processed.

We process and harmonize the simulated data from LPJmL and for the other GGCMs in the same way and following two steps, (1) we smooth the data to isolate long-term climatic trends from short-term weather variability, and (2) we harmonize output for future climate scenario data (GCMs) to outputs from an LPJmL simulation with historical climate data estimates (GSWP3-W5E5).

For (1), We use R's cubic smooth spline interpolation[64,65] over the simulated data to extract long-term trends for all outputs (vegetation, litter, and soil carbon stocks, yields, water availability, and irrigation water requirements). By taking a spline with 4 degrees of freedom per 100 years, we obtain smoothed data comparable to a 30-year running average. In (2), to be able to compare different climate scenarios to one another, we harmonize biophysical inputs for future GCM climate scenarios to an LPJmL simulation with climate input data based on observed data. We, therefore, extract the future trends and locate them on top of the baseline level for a given reference year. To avoid unrealistic amplifications of trend signals in the case of a strong underestimated baseline by the climate scenario data, we follow the method of[66], which applies a gradual transition between relative and absolute effects in the following form:

$$\widetilde{X}_{t,i}^{\text{scen}} = X_{t,i}^{\text{base}} \left(1 + \frac{\Delta X_{t-t_0,i}^{\text{scen}}}{X_{t_0,i}^{\text{base}}} \left(\frac{X_{t_0,i}^{\text{base}}}{X_{t_0,i}^{\text{scen}}} \right)^{\lambda_{t_0,i}} \right) \quad (1)$$

with

$$\Delta X_{t-t_0,i}^{\text{scen}} = X_{t,i}^{\text{scen}} - X_{t_0,i}^{\text{scen}} \quad \text{and} \quad \lambda_{t_0,i} = \begin{cases} \sqrt{\frac{X_{t_0,i}^{\text{scen}}}{X_{t_0,i}^{\text{base}}}} & X_{t_0,i}^{\text{base}} > X_{t_0,i}^{\text{scen}} \\ 1 & else \end{cases} \quad (2)$$

λ determines the degree to which the baseline is under- or overestimated and therefore controls whether the trend is applied as an absolute or relative change. For an overestimated baseline, λ is 1, which is equivalent to an entirely relative factor. For underestimated baselines, λ converges to 0 and reduces the applied relative change resulting in a mean change increasingly similar to an additive term[66]. This concept is referred to as limited calibration, as it limits the calibration to an additive term in case of a strongly underestimated baseline.

Due to data availability, the crop model projections are pre-processed using two steps, leading to a conjunction of three intervals for the calculation of MAgPIE's input crop yields: First, we use the LPJmL results for the GSWP3-W5E5 historical climate scenario as a baseline until the year 2010 (first interval). Then, harmonized results (using the limited calibration method described above) between 2010 and 2020 for LPJmL's MRI-ESM2-0 (RCP7.0) are used for the missing part of the historical trend (second interval). As it was previously described, the different GCM-GGCM projections are then joined to the historical trend from the year 2020 (third interval).

Using this approach, input crop yields diverge for different GGCMs and climate scenarios from the year 2020. This allows for comparability between data sources and scenarios.

Calibration of cropland yields to regional FAO values. Before they are used in MAgPIE, crop yields from the vegetation models are calibrated to FAO regional yield levels at the initial time step t_0. For most cases, the calibration is the ratio of the historical yields $Y_{t_0,i}^{\text{FAO}}$ reported by FAO, and regional mean yields $\overline{Y}_{t_0,i}^{\text{GGCM}}$ given historic crop area patterns and 0.5-degree yield data $Y_{t,j}^{\text{GGCM}}$ coming from the GGCMs. In these cases, a purely relative calibration is performed that only depends on the initial conditions of the starting year. However, when FAO yields are higher than yield inputs coming from the GGCMs (a so-called underestimated baseline), the relative calibration terms can lead to unrealistically large yields in the case of future yield increases. To address this issue, we determine the degree to which the baseline (FAO) is underestimated (by the parameter λ). This controls whether the calibration factor is applied as a relative factor (default case with $\lambda = 1$), as an absolute change (extreme case with $\lambda = 0$) or if it has a value in between (with

$0 < \lambda < 1$). This concept is referred to as limited calibration and follows a similar logic as the climate scenario harmonization described in the section above:

$$\widetilde{Y}_{t,j}^{\text{GGCM}} = Y_{t,j}^{\text{GGCM}} \left(1 + \frac{Y_{t_0,i}^{\text{FAO}} - \overline{Y}_{t_0,i}^{\text{GGCM}}}{Y_{t,j}^{\text{GGCM}}} \left(\frac{Y_{t,j}^{\text{GGCM}}}{\overline{Y}_{t_0,i}^{\text{GGCM}}} \right)^{\lambda_{t_0,i}} \right) \quad (3)$$

with

$$\lambda_{t_0,i} = \begin{cases} \sqrt{\frac{\overline{Y}_{t_0,i}^{\text{GGCM}}}{Y_{t_0,i}^{\text{FAO}}}} & Y_{t_0,i}^{\text{FAO}} > \overline{Y}_{t_0,i}^{\text{GGCM}} \\ 1 & else \end{cases} \quad (4)$$

Post-processing calculation of climate impacts on crop production. In MAgPIE, the production of a specific crop (Q) in scenario S is calculated as the summation of irrigated and rainfed production (Equation 5). Besides considering crop area (CA) (MAgPIE calculated) and yields (Y) (harmonized and calibrated crop yields) for both irrigation mechanisms to calculate production, we take into account the technological change factor (TC), which, as previously described, translates R&D investments into a parameter that increases yields proportionally.

$$Q^s = (\text{CA}_{rain}^s * Y_{rain}^s + \text{CA}_{irrig}^s * Y_{irrig}^s) * \text{TC}^s \quad (5)$$

To isolate the impacts of different adaptation mechanisms (changes in cropland patterns and TC specifically) on global crop production under different climate scenarios, we use the corresponding CA (rainfed and irrigated) and TC of the SSPx-NoCC scenario (no climate impacts, i.e., yields kept at 2015 values throughout the century) together with the projected Y considering impacts. This allows us to determine the effects of these suboptimal (SSPx-NoCC) conditions (together and individually) on production if no adaptation due to climate change occurs.

Self-sufficiency ratio (SSR). The self-sufficiency ratio (SSR) compares the domestic production of traded agricultural commodities of a region and its internal demand. We calculate an aggregated regional SSR as follows:

$$\text{SSR}_i = \frac{\sum_k Q_{k,i} * P_k}{\sum_k D_{k,i} * P_k} \quad (6)$$

Here $Q_{k,i}$ represents the region (i) production of the traded commodity k, P_k the 2005's world price of the commodity, which we use as aggregation weight, and $D_{k,i}$ the internal demand. We calculate the SSR in value terms to be able to compare the aggregated production-demand fraction for multiple commodities simultaneously in each region.

Shifts in crop mixes grown. The shift in crop mixes (SCM) shows which percentage of the crop mix (percentage of cropland used to produce a specific crop) is different between MAgPIE's SSP5-RCP8.5 GCM-GGCM simulations and SSP5-NoCC in the different subregions. It was calculated as follows:

$$\text{SCM}_j = \sum_{kcr} \text{PA}_{j,cc}^{kcr} - min\left(\text{PA}_{j,cc}^{kcr}, \text{PA}_{j,NoCC}^{kcr} \right) \quad (7)$$

Where PA represents the share of cropland assigned in sub-region j to crop kcr in MAgPIE simulations with climate impacts (based on GCM-GGCM data sets) (cc) or with only socioeconomic changes and without climatic effects ($NoCC$).

Data availability
The inputs used for MAgPIE runs, including the harmonized crop model projections[67]; the outputs, in GDX format, of the MAgPIE simulations[68]; and the data used to create the Figures (including those of the supplementary information)[69] are located in Zenodo.

Code availability
MAgPIE (v4.4.0) is an open-source model available at https://github.com/magpiemodel/magpie with the tag 4.4.0 (https://github.com/magpiemodel/magpie/releases/tag/v4.4.0). The model documentation for this version (4.4.0) can be found at: https://rse.pik-potsdam.de/doc/magpie/4.4.0/. Start scripts to generate the runs used in this paper, together with the plotting scripts used to generate the figures, are saved in Zenodo[70].

References
1. IPCC. *Climate Change 2021: The Physical Science Basis. Contribution of Working Group I to the Sixth Assessment Report of the Intergovernmental*

Panel on Climate Change (Cambridge University Press, Cambridge, United Kingdom and New York, NY, USA, 2021).

2. Anderson, R., Bayer, P. E. & Edwards, D. Climate change and the need for agricultural adaptation. *Curr. Opin. Plant Biol.* **56**, 197–202 (2020).

3. Challinor, A. J. et al. A meta-analysis of crop yield under climate change and adaptation. *Nat. Clim. Change* **4**, 287–291 (2014).

4. Jägermeyr, J. et al. Climate impacts on global agriculture emerge earlier in new generation of climate and crop models. *Nat. Food* **2**, 873–885 (2021).

5. IPCC. *Climate Change 2007: impacts, adaptation and vulnerability: contribution of Working Group II to the fourth assessment report of the Intergovernmental Panel* (Cambridge University Press, Cambridge, United Kingdom and New York, NY, USA, 2007).

6. Adger, W. N. Social capital, collective action, and adaptation to climate change. *Econ. Geogr.* **79**, 387–404 (2003).

7. Niles, M. T., Lubell, M. & Brown, M. How limiting factors drive agricultural adaptation to climate change. *Agriculture, Ecosyst. Environ.* **200**, 178–185 (2015).

8. Islam, M. T. & Nursey-Bray, M. Adaptation to climate change in agriculture in Bangladesh: The role of formal institutions. *J. Environ. Manag.* **200**, 347–358 (2017).

9. Stringer, L. C. et al. Adaptation and development pathways for different types of farmers. *Environ. Sci. Policy* **104**, 174–189 (2020).

10. Reilly, J. et al. Agriculture in a changing climate: impacts and adaptation. In *Climate change 1995; Impacts, adaptations and mitigation of climate change: scientific-technical analyses.*, 427–467 (Cambridge University Press, Cambridge (UK), 1996).

11. Minoli, S. et al. Global Response Patterns of Major Rainfed Crops to Adaptation by Maintaining Current Growing Periods and Irrigation. *Earth's Future* **7**, 1464–1480 (2019).

12. Lin, T. S., Song, Y., Lawrence, P., Kheshgi, H. S. & Jain, A. K. Worldwide Maize and Soybean Yield Response to Environmental and Management Factors Over the 20th and 21st Centuries. *J. Geophys. Res. Biogeosci.* **126**, e2021JG006304 (2021).

13. Zabel, F. et al. Large potential for crop production adaptation depends on available future varieties. *Glob. Change Biol.* **27**, 3870–3882 (2021).

14. Franke, J. A. et al. Agricultural breadbaskets shift poleward given adaptive farmer behavior under climate change. *Glob. Change Biol.* **28**, 167–181 (2021).

15. Jägermeyr, J. et al. Integrated crop water management might sustainably halve the global food gap. *Environ. Res. Lett.* **11**, 025002 (2016).

16. Rickards, L. & Howden, S. M. Transformational adaptation: Agriculture and climate change. *Crop Pasture Sci.* **63**, 240–250 (2012).

17. Smit, B. & Skinner, M. W. Adaptation options in agriculture to climate change: A typology. *Mitigation Adapt. Strat. Glob. Change* **7**, 85–114 (2002).

18. Huang, H., von Lampe, M. & van Tongeren, F. Climate change and trade in agriculture. *Food Policy* **36**, S9–S13 (2011).

19. Quiggin, J. & Horowitz, J. Costs of adjustment to climate change. *Australian J. Agricul. Res. Econ.* **47**, 429–446 (2003).

20. Janssens, C. et al. Global hunger and climate change adaptation through international trade. *Nat. Clim. Change* **10**, 829–835 (2020).

21. Mosnier, A. et al. Global food markets, trade and the cost of climate change adaptation. *Food Security* **6**, 29–44 (2014).

22. Stevanović, M. et al. The impact of high-end climate change on agricultural welfare. *Sci. Adv.* **2**, e1501452 (2016).

23. Randhir, T. O. & Hertel, T. W. Trade Liberalization as a Vehicle for Adapting to Global Warming. *Agri. Res. Econ. Rev.* **29**, 159–172 (2000).

24. Delincé, J., Ciaian, P. & Witzke, H.-P. Economic impacts of climate change on agriculture: the AgMIP approach. *J. Appl. Remote Sensing* **9**, 097099 (2015).

25. Nelson, G. C. et al. Climate change effects on agriculture: Economic responses to biophysical shocks. *Proc. Natl. Acad. Sci. USA.* **111**, 3274–3279 (2014).

26. Popp, A. et al. Land-use futures in the shared socio-economic pathways. *Glob. Environ. Change* **42**, 331–345 (2017).

27. Lobell, D. B., Baldos, U. L. C. & Hertel, T. W. Climate adaptation as mitigation: The case of agricultural investments. *Environ. Res. Lett.* **8**, 015012 (2013).

28. Iizumi, T. et al. Climate change adaptation cost and residual damage to global crop production. *Clim. Res.* **80**, 203–218 (2020).

29. Frieler, K. et al. Assessing the impacts of 1.5°C global warming - simulation protocol of the Inter-Sectoral Impact Model Intercomparison Project (ISIMIP2b). *Geoscientific Model Develop. Discuss.* **12**, 4321–4345 (2016).

30. Dietrich, J. P. et al. MAgPIE 4-a modular open-source framework for modeling global land systems. *Geoscientific Model Develop.* **12**, 1299–1317 (2019).

31. Dietrich, J. P. et al. MAgPIE - An Open Source land-use modeling framework - Version 4.4.0 https://github.com/magpiemodel/magpie (2021).

32. Iizumi, T. et al. Crop production losses associated with anthropogenic climate change for 1981-2010 compared with preindustrial levels. *Int. J. Climatol.* **38**, 5405–5417 (2018).

33. Balkovič, J. et al. Global wheat production potentials and management flexibility under the representative concentration pathways. *Glob. Planetary Change* **122**, 107–121 (2014).

34. Von Bloh, W. et al. Implementing the nitrogen cycle into the dynamic global vegetation, hydrology, and crop growth model LPJmL (version 5.0). *Geoscientific Model Develop.* **11**, 2789–2812 (2018).

35. Lutz, F. et al. Simulating the effect of tillage practices with the global ecosystem model LPJmL (version 5.0-tillage). *Geoscientific Model Develop.* **12**, 2419–2440 (2019).

36. Okada, M. et al. Varying benefits of irrigation expansion for crop production under a changing climate and competitive water use among crops. *Earth's Future* **6**, 1207–1220 (2018).

37. Haas, E. et al. LandscapeDNDC: A process model for simulation of biosphere-atmosphere-hydrosphere exchange processes at site and regional scale. *Landsc. Ecol.* **28**, 615–636 (2013).

38. Liu, W. et al. Global investigation of impacts of PET methods on simulating crop-water relations for maize. *Agri. Forest Meteorol.* **221**, 164–175 (2016).

39. Zabel, F. et al. Global impacts of future cropland expansion and intensification on agricultural markets and biodiversity. *Nat. Commun.* **10**, 2844 (2019).

40. Hank, T. B., Bach, H. & Mauser, W. Using a remote sensing-supported hydro-agroecological model for field-scale simulation of heterogeneous crop growth and yield: Application for wheat in central Europe. *Remote Sensing* **7**, 3934–3965 (2015).

41. Mauser, W. et al. Global biomass production potentials exceed expected future demand without the need for cropland expansion. *Nat. Commun.* **6**, 8946 (2015).

42. Dietrich, J. P., Schmitz, C., Lotze-Campen, H., Popp, A. & Müller, C. Forecasting technological change in agriculture-An endogenous implementation in a global land use model. *Technological Forecasting Soc. Change* **81**, 236–249 (2014).

43. Houghton, R. A. et al. Carbon emissions from land use and land-cover change. *Biogeoscience* **9**, 5125–5142 (2012).

44. Schipper, E. L. F. Maladaptation: When Adaptation to Climate Change Goes Very Wrong. *One Earth* **3**, 409–414 (2020).

45. Zhao, C. et al. Temperature increase reduces global yields of major crops in four independent estimates. *Proc. Natl. Acad. Sci. USA.* **114**, 9326–9331 (2017).

46. Müller, C. et al. Exploring uncertainties in global crop yield projections in a large ensemble of crop models and CMIP5 and CMIP6 climate scenarios. *Environ. Res. Lett.* **16**, 034040 (2021).

47. Pokorny, B., de Jong, W., Godar, J., Pacheco, P. & Johnson, J. From large to small: Reorienting rural development policies in response to climate change, food security and poverty. *Forest Policy Econ.* **36**, 52–59 (2013).

48. Osendarp, S. et al. Act now before Ukraine war plunges millions into malnutrition. *Nature* **604**, 620–624 (2022).

49. Bodirsky, B. L. et al. Integrating degrowth and efficiency perspectives enables an emission-neutral food system by 2100. *Nat. Food.* **3**, 341–348 (2022).

50. Stevanović, M. et al. Mitigation Strategies for Greenhouse Gas Emissions from Agriculture and Land-Use Change: Consequences for Food Prices. *Environ. Sci. Technol.* **51**, 365–374 (2017).

51. O'Neill, B. C. et al. The roads ahead: Narratives for shared socioeconomic pathways describing world futures in the 21st century. *Glob. Environ. Change* **42**, 169–180 (2017).

52. Bodirsky, B. L. et al. The ongoing nutrition transition thwarts long-term targets for food security, public health and environmental protection. *Scientific Rep.* **10**, 19778 (2020).

53. Baumstark, L. et al. REMIND2.1: transformation and innovation dynamics of the energy-economic system within climate and sustainability limits. *Geoscientific Model Develop.* **14**, 6571–6603 (2021).

54. Schaphoff, S. et al. LPJmL4 - A dynamic global vegetation model with managed land - Part 1: Model description. *Geoscientific Model Develop.* **11**, 1343–1375 (2018).

55. van Vuuren, D. P. et al. The representative concentration pathways: An overview. *Clim. Change* **109**, 5–31 (2011).

56. Riahi, K. et al. The Shared Socioeconomic Pathways and their energy, land use, and greenhouse gas emissions implications: An overview. *Global Environ. Change* **42**, 153–168 (2017).

57. Warszawski, L. et al. The inter-sectoral impact model intercomparison project (ISI-MIP): Project framework. *Proc. Natl. Acad. Sci. USA* **111**, 3228–3232 (2014).

58. ISIMIP. ISIMIP Repository https://www.isimip.org/outputdata/isimip-repository/ (2022).

59. Cucchi, M. et al. WFDE5: Bias-adjusted ERA5 reanalysis data for impact studies. *Earth System Sci. Data* **12**, 2097–2120 (2020).

60. Lange, S. WFDE5 over land merged with ERA5 over the ocean (W5E5). V. 1.0. [Data set]. https://doi.org/10.5880/pik.2019.023 (2019).

61. Lange, S. Trend-preserving bias adjustment and statistical downscaling with ISIMIP3BASD (v1.0). *Geoscientific Model Develop.* **12**, 3055–3070 (2019).

62. Ray, D. K., Gerber, J. S., Macdonald, G. K. & West, P. C. Climate variation explains a third of global crop yield variability. *Nat. Commun.* **6**, 5989 (2015).

63. Mengel, M., Treu, S., Lange, S. & Frieler, K. ATTRICI v1.1 - Counterfactual climate for impact attribution. *Geoscientific Model Develop.* **14**, 5269–5284 (2021).

64. Ripley, B. D. & Maechler, M. smooth.spline: Fit a Smoothing Spline https://www.rdocumentation.org/packages/stats/versions/3.6.2/topics/smooth.spline (2022).

65. Hastie, T. & Tibshirani, R.*Generalized Additive Models*, vol. 43 (Chapman Hall & CRC, 1990).

66. Heinke, J. et al. A new climate dataset for systematic assessments of climate change impacts as a function of global warming. *Geoscientific Model Develop.* **6**, 1689–1703 (2013).

67. Molina Bacca, E. J. MAgPIE model input data sets: Climate change-driven global land-use system adaptation under CMIP6-based crop model projections [Data set]. Zenodo. https://doi.org/10.5281/zenodo.7228383 (2022).

68. Molina Bacca, E. J. MAgPIE model runs outputs: Climate change-driven global land-use system adaptation under CMIP6-based crop model projections [Data set]. Zenodo. https://doi.org/10.5281/zenodo.7233619 (2022).

69. Molina Bacca, E. J. Magpie model runs csv for plotting: Climate change-driven global land-use system adaptation under CMIP6-based crop model projections. (Version V2) [Data set]. Zenodo. https://doi.org/10.5281/zenodo.8178516 (2023).

70. Molina Bacca, E. J. Start and plotting scripts: Climate change-driven global land-use system adaptation under CMIP6-based crop model projections. (Version V2) [Data set]. Zenodo. https://doi.org/10.5281/zenodo.8177495 (2023).

71. KC, S. & Lutz, W. The human core of the shared socioeconomic pathways: Population scenarios by age, sex and level of education for all countries to 2100. *Glob. Environ. Change* **42**, 181–192 (2017).

72. Dellink, R., Chateau, J., Lanzi, E. & Magné, B. Long-term economic growth projections in the Shared Socioeconomic Pathways. *Glob. Environ. Change* **42**, 200–214 (2017).

73. Strefler, J. et al. Alternative carbon price trajectories can avoid excessive carbon removal. *Nat. Commun.* **12**, 2264 (2021).

Competing interests

The authors declare no competing interests.

Additional information

Supplementary information The online version contains supplementary material available at https://doi.org/10.1038/s43247-023-00941-z.

Correspondence and requests for materials should be addressed to Edna J. Molina Bacca.

Peer review information *Communications Earth & Environment* thanks Neal Hughes and the other, anonymous, reviewer(s) for their contribution to the peer review of this work. Primary Handling Editors: Martina Grecequet and Aliénor Lavergne. A peer review file is available.

Reprints and permission information is available at http://www.nature.com/reprints

Publisher's note Springer Nature remains neutral with regard to jurisdictional claims in published maps and institutional affiliations.